ELSEVIER

Catalysis Today 24 (1995) 87–93

CATALYSIS
TODAY

Modelling of a trickle bed reactor with strong exothermal reaction

Jiří Hanika*, Jiří Růžička

Institute of Chemical Technology Prague, 166 28 Prague 6, Czech Republic

Abstract

In this study the solution of the model for the single particle vertical string of catalyst spheres is compared to the experimental data obtained for cyclohexene hydrogenation over a palladium active carbon supported extruded catalyst. Special attention was paid to the concentration distribution of the gaseous component in the flowing film of the reaction mixture and inside the catalyst pellets along the string.

1. Introduction

In many situations the behaviour of the trickle bed reactors is influenced by a liquid reaction mixture maldistribution which makes possible a formation of dry zones or even hot spots when a strongly exothermal reaction occurs in a reaction system. Fundamental investigations of heat and mass transfer effects on a reaction proceeded in a porous catalyst particle trickled with liquid under defined hydrodynamic conditions are usually carried out utilizing a simplified theoretical model that consists of the vertical string of spherical catalyst particles. In papers [1,2], this model was firstly employed for an isothermal case study. The extended non-isothermal model solved in the paper [3] can serve as a simple tool for the evaluation of the effects of a liquid film thickness change and a partial liquid evaporation with respect to internal temperature gradients of a catalyst pellet and for estimation of the hot spot appearance in the trickle bed reactors, which were recently observed [4].

There are several mathematical models of completely [1–3] or partially [5–8] wetted catalyst particles which may exist in the trickle bed reactors. Each of those models is based on many assumptions and is forced to use simplifications in order to solve the complex equation systems. Only few experiments were carried out to elucidate the relation of heat and mass transfers under defined hydrodynamic circumstances close to those of the trickle bed reactors [1,9]. These experiments were focused on measurements of overall conversion under well defined wetting effectiveness and scarce data on heat transfer were obtained.

In order to investigate heat transfer among and within the catalyst particles in the trickle beds, it is necessary to construct a string of the catalyst particles with a temperature detection in different locations, and a non-destructive fixation. Experiments arranged in such a way confirmed a pseudo-isothermal behaviour of the catalyst string during the liquid phase reaction regime [9].

---

* Corresponding author.

SSDI 0920-5861(95)00004-6

2. Theoretical

2.1. Assumptions of reactor model

(1) Let us consider a steady, pseudo-isothermal, and isobaric system consisting of a vertical column of porous spheres having constant radii in gas (hydrogen) atmosphere, wetted by a liquid reaction mixture containing dissolved gas, hydrogenated substrate, and reaction product. (2) The liquid flows down the external surface of spherical porous catalyst particles in the form of a laminar film. (3) The liquid is introduced on the first sphere with uniform inlet concentration of dissolved gas. (4) The concentration of the dissolved gas in the film at the gas–liquid interphase is equal to its equilibrium value for a given temperature and pressure. (5) The transport of gas across the film is induced by diffusion and in the direction of the film flow by convection only (diffusion transport in the direction of the film flow can be neglected). (6) The reaction taking place in the catalytically active porous sphere is irreversible, of first order with respect to the dissolved gas and of zero order with respect to hydrogenated substrate. (7) The region of contact in between two adjacent spheres, filled with liquid meniscus is symmetric with respect to a horizontal plane through the contact point and its liquid volume is stagnant. (8) The average thickness of the film is of several orders of magnitude smaller than the radius of the sphere.

2.2. Convective diffusion in flowing film

The mass balance written for a volume element of the liquid in the film (see [2,3]) in dimensionless form yields following partial differential equation governing the pseudo-isothermal mass transfer:

$$\left(\frac{\partial^2 Y}{\partial \rho^2}\right) + N_{\mathrm{Pe}}P(\rho^2 - 1)\sin^{-5/3}(\vartheta)\left(\frac{\partial Y}{\partial \vartheta}\right) = 0 \quad (1)$$

Eq. (1) has to be supplemented with boundary conditions according to the assumptions determining the solution of the problem:

$$Y(\rho,\vartheta_0) = Y_0(\rho) \quad (2)$$

$$Y(0,\vartheta) = 1 \quad (3)$$

$$\left(\frac{\partial Y}{\partial \rho}\right)_{\rho=1} = -\Phi_{\mathrm{ex}}\sin^{-2/3}(\vartheta)Y(1,\vartheta) \quad (4)$$

in which $\rho\epsilon\langle 0,1\rangle$ and $\vartheta\epsilon\langle \vartheta_0, \pi - \vartheta_0\rangle$.

2.3. Internal mass and heat transfer in catalyst sphere

Simultaneous diffusion and exothermal reaction inside the catalyst pellet for an adiabatic situation can be described in spherical coordinates:

$$\frac{\partial^2 Y}{\partial \rho^2} + \frac{2}{\rho}\frac{\partial Y}{\partial \rho} + \frac{1}{\rho^2 \sin(\vartheta)}\frac{\partial}{\partial \vartheta}\left(\sin(\vartheta)\frac{\partial Y}{\partial \vartheta}\right) = \Phi_{\mathrm{in}}^2 Y \exp\left(\frac{\gamma\beta(1-Y)}{1+\beta(1-Y)}\right) \quad (5)$$

Boundary conditions correspond to the assumptions of the model:

$$\rho = 0 \quad (\partial Y/\partial \rho) = 0 \quad (6)$$

$$\rho = 1 \quad Y(1,\vartheta) = 1 - \Delta + \Delta\cos(\vartheta) \quad (7)$$

The relation between temperature and concentration for the adiabatic case is defined by following invariant:

$$\theta = \gamma\beta(1-Y) \quad (8)$$

where β and γ are dimensionless heat of reaction parameter and activation energy, respectively. Thus, the pseudo-isothermal solution for an individual spherical catalyst pellet can be extended to the non-isothermal string of catalyst pellets by the step by step change of the inlet temperature from one sphere to the next one depending on the extent of the reaction conversion and heat release on previous upper catalyst pellets.

2.4. Numerical solution

The system of parabolic and elliptic partial differential equations was solved using the finite difference method. The solution accuracy was

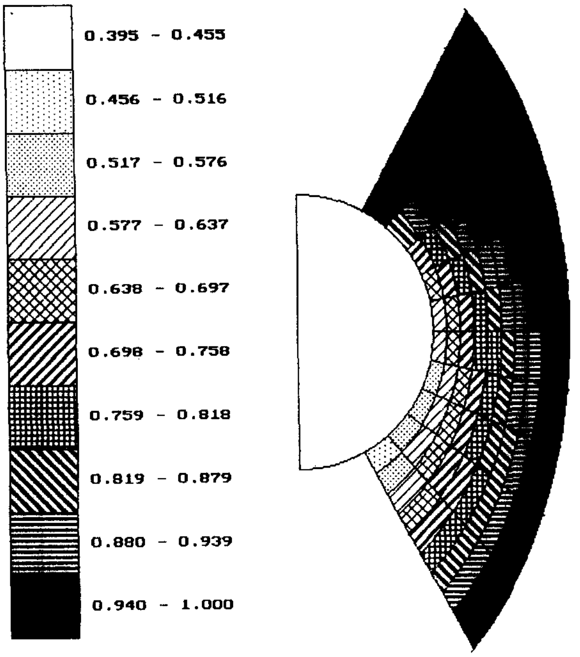

Fig. 1. Concentration fields in liquid film. $Y_0=1$; $N_{Pe}P=3.9$; $\beta=0.02$; $\gamma=7$; Φin = 15; $\eta_{in}=0.13$; Φex = 1.3; $\eta_{ex}=0.54$.

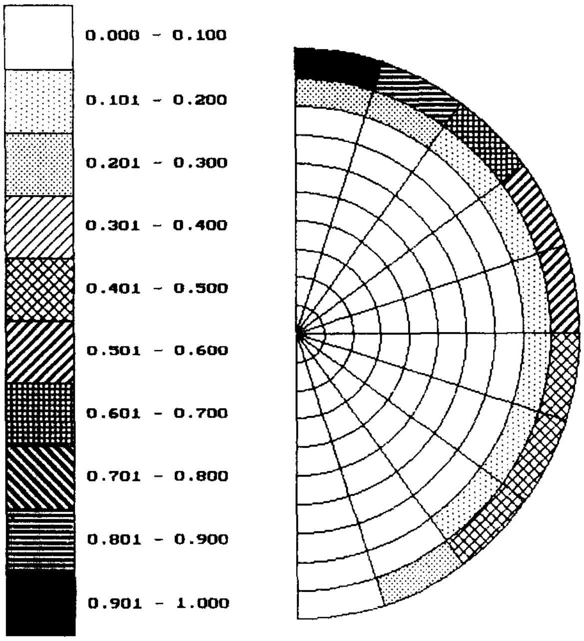

Fig. 2. Concentration fields inside the first spherical catalyst pellet. $Y_0=1$; $N_{Pe}P=3.9$; $\beta=0.02$; $\gamma=7$; Φin = 15; $\eta_{in}=0.13$; Φex = 1.3; $\eta_{ex}=0.54$.

checked using the half step procedure applied both to the liquid film and the catalyst sphere.

The model was solved for the string of several catalyst spheres until the concentration profiles reached their equilibrium values. The examples of concentration fields both outside and inside the first catalyst pellet computed with input data based on our experimental conditions are given in Figs. 1 and 2. The corresponding equatorial concentration profiles both in the flowing film and in the catalyst pellet are given in Figs. 3 and 4. Similar results were given by the model solution for next spheres in the string.

The effectiveness factor of external diffusion limitation in flowing film follows from the concentration profile along the external surface of the catalyst pellet, thus:

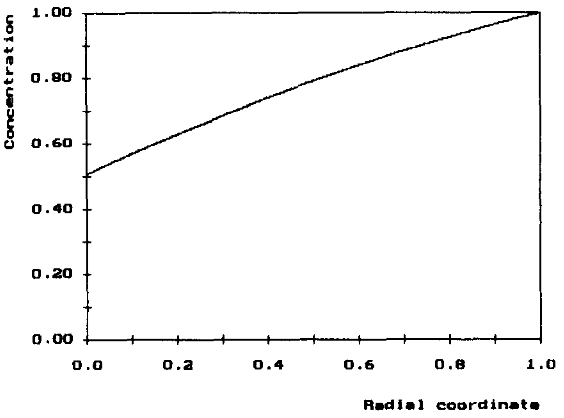

Fig. 3. Equatorial concentration profile in liquid film on first catalyst pellet (parameters see Fig. 1).

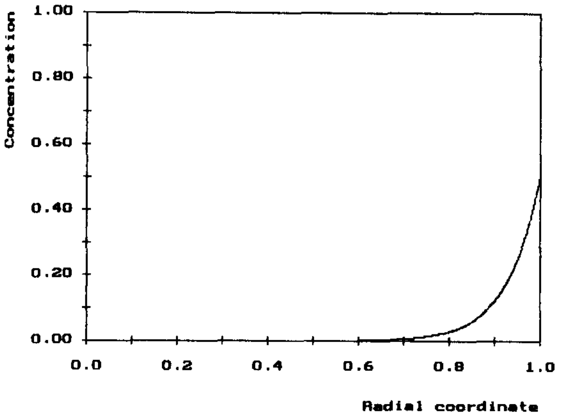

Fig. 4. Equatorial concentration profile inside first catalyst pellet (parameters see Fig. 2).

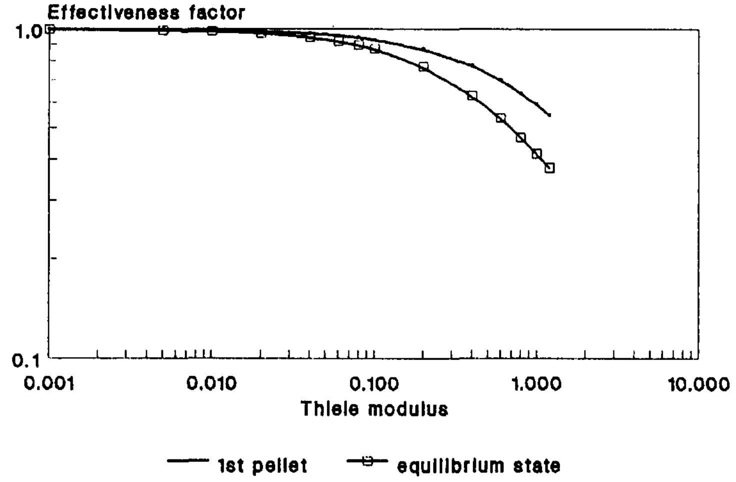

Fig. 5. External effectiveness factor versus Thiele modulus for first and *n*th pellets (other parameters see Fig. 1).

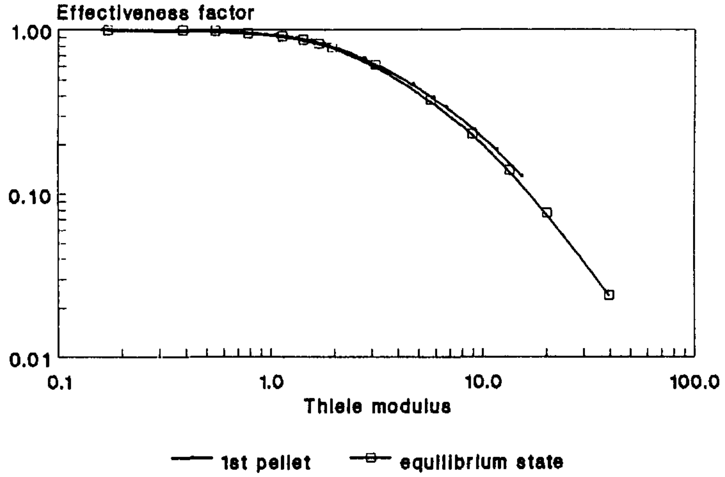

Fig. 6. Internal effectiveness factor versus Thiele modulus for first and *n*th pellets (other parameters see Fig. 2)

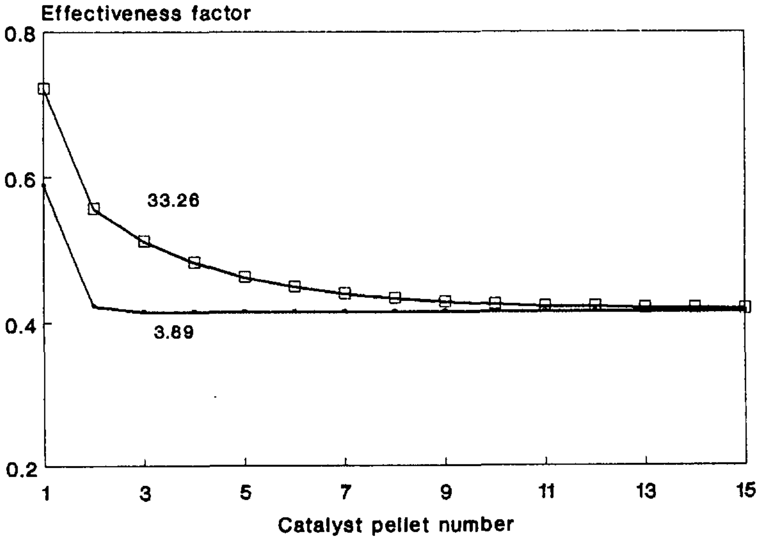

Fig. 7. External effectiveness factor along string of catalyst pellets for different values of product $N_{Pe}P$.

$$\eta_{ex}=\frac{1}{2}\int_{0}^{\pi} Y[1,\vartheta]\sin(\vartheta)\mathrm{d}\vartheta \tag{9}$$

Similarly an effectiveness factor for internal diffusion can be evaluated from the concentration field inside the sphere:

$$\eta_{in}=\frac{2\int_{0}^{\pi}\left(\frac{\partial Y}{\partial \rho}\right)_{\varrho=1}\sin(\vartheta)\mathrm{d}\vartheta}{\Phi_{in}^{2}\int_{0}^{\pi} Y[1,\vartheta]\exp\left[\frac{\gamma\beta(1-Y[1,\vartheta])}{1+\beta(1-Y[1,\vartheta])}\right]\sin^{3}(\vartheta)\mathrm{d}\vartheta} \tag{10}$$

Values of both integrals were computed using the trapezoid procedure.

The dependencies of the effectiveness factors on external and internal Thiele moduli for the experimental system are plotted in Figs. 5 and 6, respectively. The results correspond to the isothermal model solution for both the first and the *n*th spheres in the string where the effectiveness factors reached their equilibrium values. The example of reaching the equilibrium state for the string of the catalyst pellets is given in Fig. 7, where the lower curve belongs to experiments made in this study. It is clear, when the liquid flow rate is five times increased, i.e. there are Peclet numbers and the simplex P for the product is increased, the system reaches the equilibrium regime much more slowly, see the upper curve in Fig. 7. The influence of this product on the internal effectiveness factor is very slight.

Table 1
Comparison of experimental and numerical data

Parameter	Model solution		Experimental
	First sphere	*n*th sphere	
Φ_{ex}	1.25	1.25	–
η_{ex}	0.54	0.37	0.40
Φ_{in}	15	53	–
η_{in}	0.13	0.013	0.014
K (m/s)	5.7×10^{-10}	5.7×10^{-10}	12.0×10^{-10}

$N_{Pe}P=3.9$; $\beta=0.02$; $\gamma=7.1$; $R=2.8$ mm; $D_{eff}=D/10$; $D=2\times10^{-8}$ m²/s.

There is a solution of the adiabatic reaction regime for the first sphere given demonstrated in Fig. 8, showing dependencies of internal effectiveness factor on Thiele modulus. It is clear that the increase of the value of the parameter β enables an initiation of the catalyst particle centre overheating and under certain circumstances a formation of multiple steady states in the catalyst pellet is possible. But in the liquid reaction regime which was experimentally investigated in this study the reaction heat parameter β reached the very low value of 0.02 for which the multiple steady states and the hysteretic behaviour do not exist.

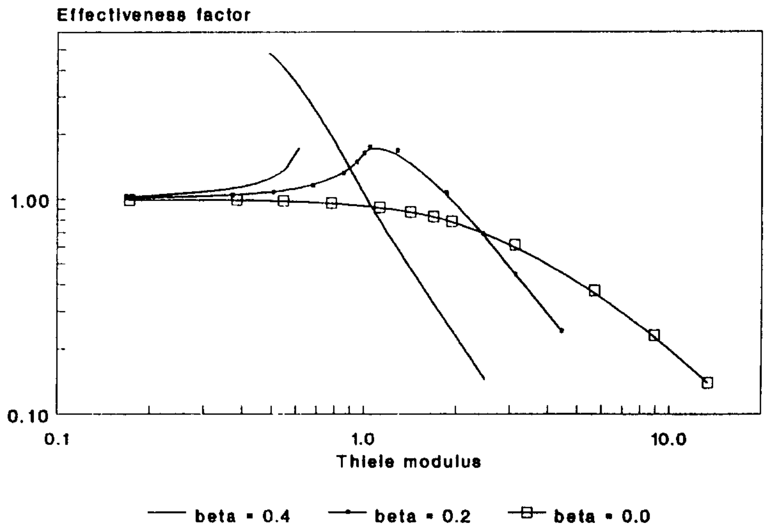

Fig. 8. Internal effectiveness factor versus Thiele modulus for different values of reaction heat parameter.

3. Experimental

3.1. Apparatus and reaction conditions

Theoretical results were confronted to experiments in which the hydrogenation of cyclohexene on palladium on the charcoal catalyst (3% Pd/C, cylindrical extrudates, length 9 mm, diameter 4 mm) was used as a model reaction. Kinetics of this reaction were studied in detail in previous papers [10–12] and corresponded to the assumptions mentioned above. The trickle bed reactor consisted in a fixative wire spiral of a triangular cross section in which the catalyst extrudates (25) are placed. The thermostated glass jacket of the reactor enables to control visually the wetting efficiency of the extrudates. Gas–liquid feed inlet (hydrogen max. 30 l/h and cyclohexene 1 mol/h) was led through a needle to the top of the first extrudate. Cyclohexene was typically used in concentration of 100%, and the string of the particles was wetted by cyclohexane prior to the reaction. All runs were carried out in the temperature range from 50 through 80°C, and under atmospheric pressure. Under such conditions the extrudates were completely wetted. Temperatures were measured by means of thermocouples made of copper–constantan wires connected with a digital data logger. Cyclohexene conversion was determined by routine GLC analysis. The model trickle bed reactor was described in detail in [9].

3.2. Comparison to model solution

The mathematical model was solved for the radius of the sphere with equivalent volume to catalyst extrudate; other data relating to experimental conditions are given in Table 1. The only adjustable parameter was the kinetic constant of hydrogenation. Comparison of the measured apparent kinetic constant value to the theoretical one, for which computed effectiveness factors of external and internal diffusion were closed to the experimental data [10–12] is shown in Table 1. It is seen from the results that the experimentally determined kinetic constant is somewhat higher. This is due to slightly different arrangements of the experiment which data are being compared. There were catalyst extrudates of cylindrical shape and with a nonuniform radial palladium distribution inside them used for the experiments. Both the model solution and the experimental results showed that the hot spots observed in the trickle bed reactors probably are not formed as a result of heat and mass transfer effects on liquid phase reaction but they are likely the product of the liquid reaction mixture maldistribution which makes possible to form the dry unwetted catalyst pellets on which the reaction between volatile substrate and gaseous component can proceed. The transition of the reaction to the gas phase regime is supported by the sudden increase of the diffusion coefficient and of the reaction heat parameter. Similar conclusions were drawn in ref. [3].

4. Conclusions

The strong mass transfer limitation of the reaction proceeding in liquid phase suppresses the formation of steep temperature gradients inside the catalyst pellets. Thus, the pseudo-isothermal model, solved in this paper, adequately describes the behaviour of the catalyst pellets under liquid film cover.

During experiments there was no evidence about the formation of partially wetted catalyst pellets even though the cyclohexene hydrogenation represents a strong exothermal reaction ($\Delta H = -112.5$ kJ/mol).

5. Symbols

c_0	feed concentration (mol/m^3)
D, D_{eff}	diffusion coefficient in film and catalyst, respectively (m^2/s)
E	activation energy (kJ/mol)

ΔH	reaction enthalpy (kJ/mol)
K, K'	reaction rate constant related to sphere geometric and specific surface, respectively (m/s)
$N_{Pe} = W_0 S_0/D$	Peclet number
$P = S_0/R$	geometrical simplex
r	radial coordinate (m)
R	sphere radius or gas constant (m or kJ/mol K)
T_0	inlet temperature (K)
S_0	equatorial (minimal) thickness of film (m)
W_0	equatorial (maximal) phase velocity of liquid (m/s)
$Y = c/c_0$	dimensionless concentration
$\beta = c_0(-\Delta H) D_{eff}/\lambda_{eff} T_0$	reaction heat parameter
$\gamma = E/RT_0$	dimensionless activation energy
$\Delta = [Y(1,0) - Y(1,\pi)]/2R$	external concentration gradient
η_{ex}, η_{in}	effectiveness factor of external and internal diffusion, respectively
ϑ, ϑ_0	angular coordinate, of meniscus
$\theta = E(T - T_0)/RT_0$	dimensionless temperature
λ_{eff}	effective thermal conductivity of sphere (W/m K)
$\rho = r/S_0$ or r/R	dimensionless coordinate
$\Phi_{ex} = K S_0/D$	external Thiele modulus
$\Phi_{in} = R\sqrt{(K'/D_{eff})}$	internal Thiele modulus

References

[1] C.N. Satterfield, A.A. Pelossof and T.K. Sherwood, AIChE J., 15 (1969) 226.

[2] J. Hanika, K. Sporka and V. Růžička, Collect. Czech. Chem. Commun., 36 (1971) 1358.

[3] A. Hrovat and J. Levec, Chem. Eng. Commun., 85 (1989) 49.

[4] J.Hanika and V. Staněk, Stud. Surf. Sci. Catal., 27 (1986) 547.

[5] P.L. Mills, S. Lai, M.P. Dudukovič and P.A. Ramachandran, Ind. Eng. Chem. Res., 27 (1988) 191.

[6] M.P. Harold, Chem. Eng. Sci., 43 (1988) 3197.

[7] M.P. Harold, AIChE J., 34 (1988) 980.

[8] M.P. Harold and K.M. Ng, AIChE J., 33 (1987) 1448.

[9] J. Růžička and J. Hanika, Catal. Today, 92 (1994) 467.

[10] J. Hanika, K. Sporka, V. Růžička and J. Krausová, Chem. Eng. Commun., 2 (1975) 19.

[11] J. Hanika and K. Sporka, Chem. Prům., 34 (1984) 182.

[12] J. Hanika and V. Ehlová, Coll. Czech. Chem. Commun., 54 (1989) 3003.